SLS-Note 3/95
April 1995

2D Study of the SLS Storage Ring Quadrupoles

D.C. George & V. Vranković

PSI

THE SWISS SYNCHROTRON LIGHT SOURCE

1 Introduction

The quadrupoles for the SLS storage ring will have an aperture radius of $30\,mm$ and a nominal field gradient of $22\,T/m$. There are three quadrupole types with effective field lengths of 200, 280 and $350\,mm$. The good field region extends horizontally to $\pm 30\,mm$ and vertically to $\pm 20\,mm$. This study optimizes the pole shape to determine the best attainable field quality for the given boundary conditions. The vacuum chamber design is the starting point for this study. The results are very much dependent on the space available.

To accommodate the antechamber, the quadrupoles need to be made in two separate halves mechanically connected together on one side only. Sufficient space for the vacuum pumps has to be left on the open side. A possible yoke geometry including coils is proposed.

2 Pole-tip profile

This study uses a pole-tip contour which is a smooth curve. The central part is a fixed hyperbola. The ends are described by a cubic spline extending smoothly from the hyperbola and passing through three points (Fig-1). The end point is constrained to follow the tapered pole side. During the automatic optimization process, the points are moved to obtain the best result.

The magnetic fields are calculated using the POISSON 2D program. The model for the rest of the magnet is highly simplified (Fig-2) in order to be able to perform the calculations in a reasonable time. Since the results should be good over the whole excitation range, the field calculation is performed both for real iron and also for iron with infinite permeability. About one hundred iterations were generally needed to reach a solution.

The criteria used to test the quality of solution is the RMS deviation of the vector potential solution A as calculated with POISSON, from the ideal quadrupole gradient G_0:

$$RMS = \sum_{ellipse} \{A - [-\tfrac{G_0}{2}(x^2 - y^2)]\}^2$$

It is sufficient to take the vector potential on a set of points lying on an ellipse that surrounds the good field region (Fig-3).

3 Coil

Since the good field region is not symmetric, it is possible to cut back the pole on one side without any loss of field quality (Fig-4). This allows the use of a larger coil with less power consumption ($\sim 15\%$). Each end is then optimized separately. A symmetrical solution may however be preferable because of other considerations such as forces.

The nominal pole-tip field is $6.6\,kGauss$. For the worst case we expect $\sim 2\%$ saturation and another $\sim 3\%$ as a safety margin. The required excitation is then:

$$NI \approx 1.05 \times \frac{B_0 R_0}{2\mu_0} \approx 8'273\,AmpereTurns/pole$$

The coil is water-cooled with 21 turns wound in two layers. Hollow copper conductor is used. The conductor cross-section is square ($a = 8\,mm$) with a round cooling hole ($d = 3.5\,mm$). The expected maximum values for the single quadrupoles are $395\,Amperes$, $13.5\,Volts$, $5.3\,kW$. Even the largest family
(24 quads with $L_{eff} = 280\,mm$) will not exceed $300\,Volts$.

4 Pole-base and yoke

The pole base is tilted away from the mid-plane. This allows enough space for the vacuum pump. The coils as shown could be mounted and dismounted without having to split the yoke and lose mechanical stability (Fig-5a:d). The pole-base asymmetry has no influence on the field quality.

5 Results

The field for the full model with the complete geometry (Fig-6) was recalculated with the POISSON program using a filling factor of 0.85 to compensate for the end fields for shortest quadrupole type.

The deviation from a perfect quadrupole field for nominal excitation is shown in Figs-7,8a:c. The magnet is practically linear (Fig-9) and the field quality is independent of the excitation level (Figs-10).

6 Closing remarks

A comparison with similar quadrupoles from other light sources is shown in Fig-11. We must not forget that, although the errors are very small on paper, the actual field quality will probably be dominated by the tolerances. The 3D end fields also remain to be solved.

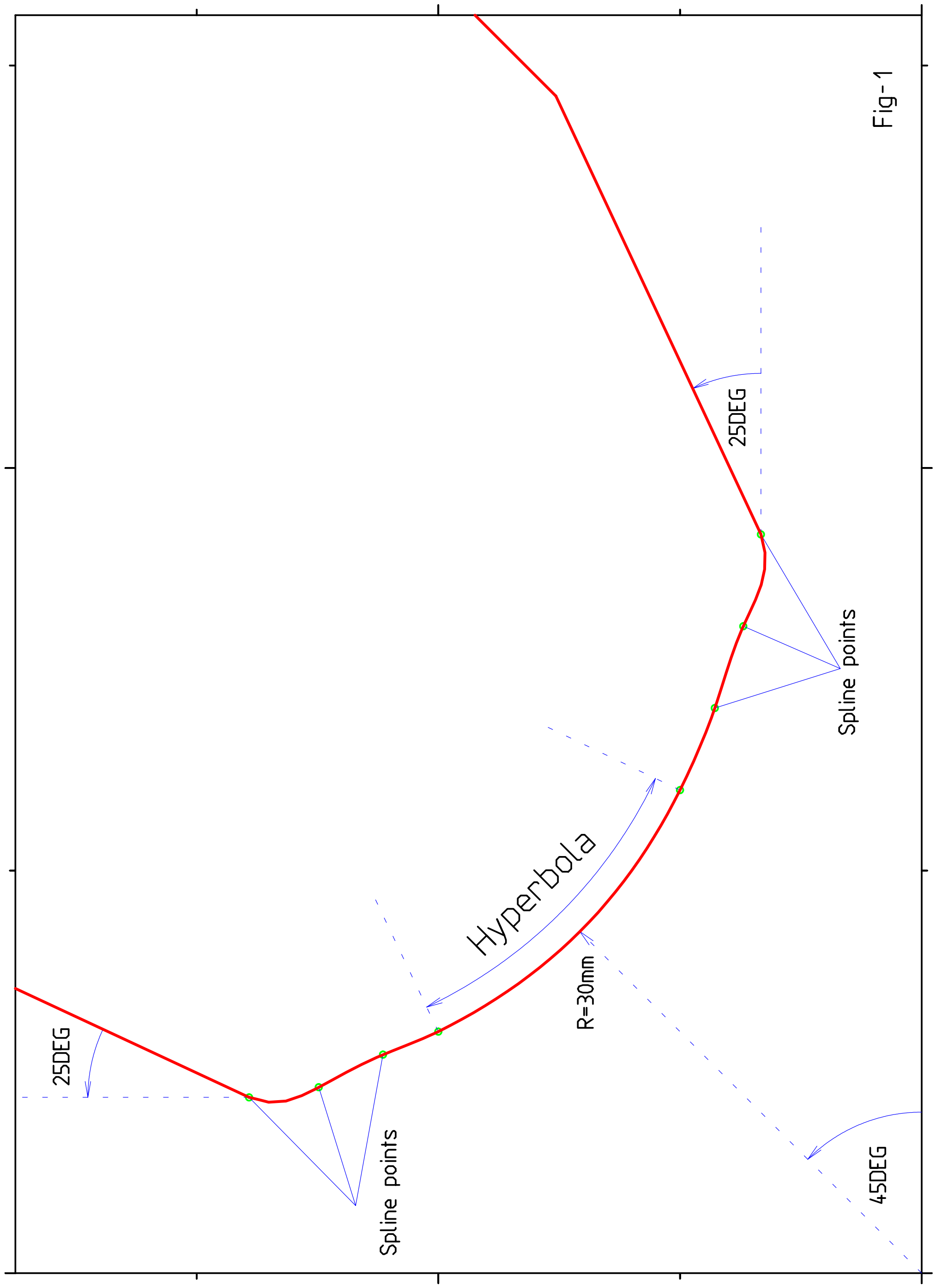
25DEG
Spline points
3
Hyperbola
R=30mm
25DEG
Spline points
45DEG
0
0
5
Fig-1

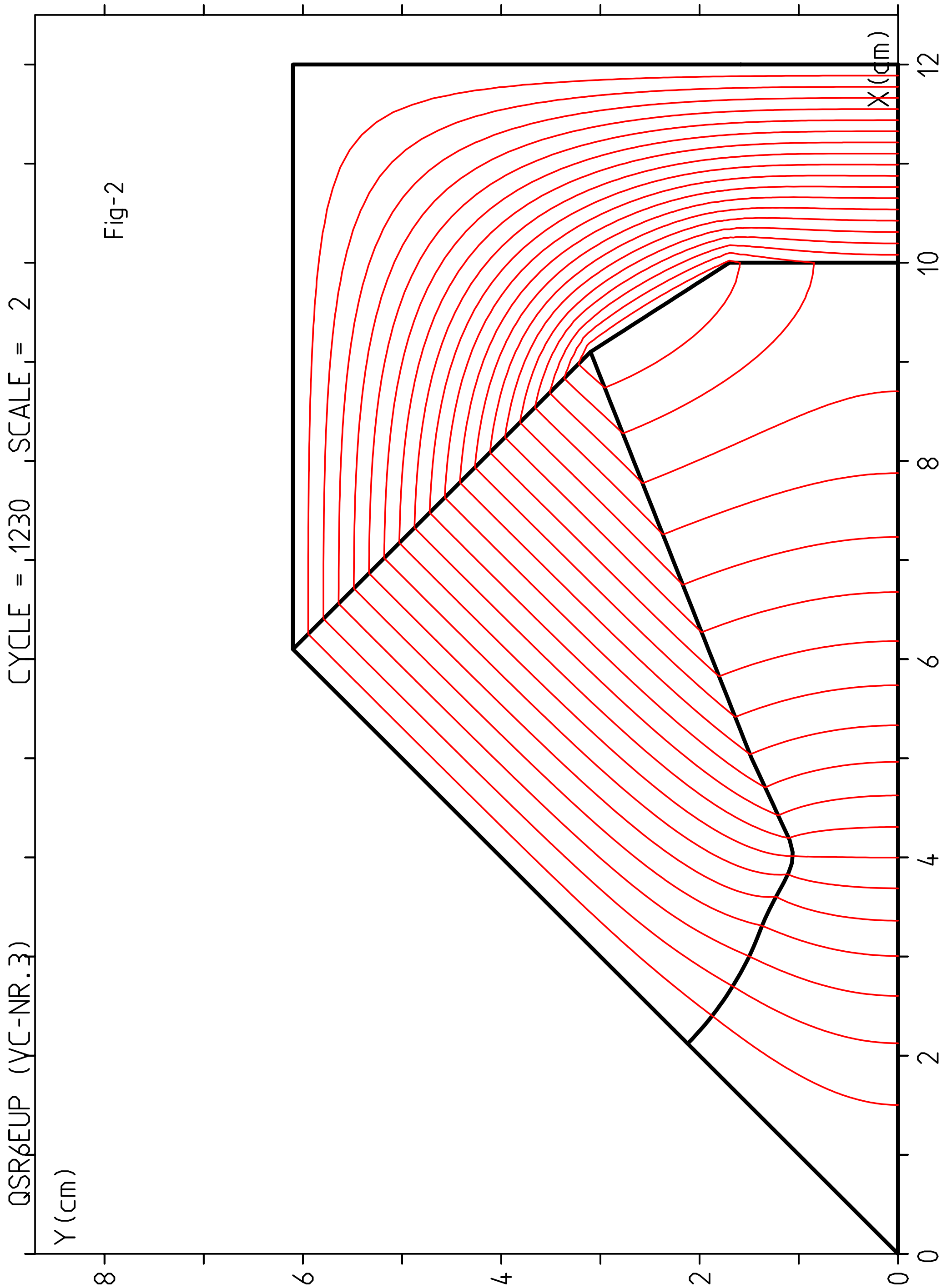

QSR6EUP (YC-NR.3)
CYCLE = 1230 SCALE = 2
Fig-2
Y (cm)
X (cm)
0
2
4
6
8
10
12

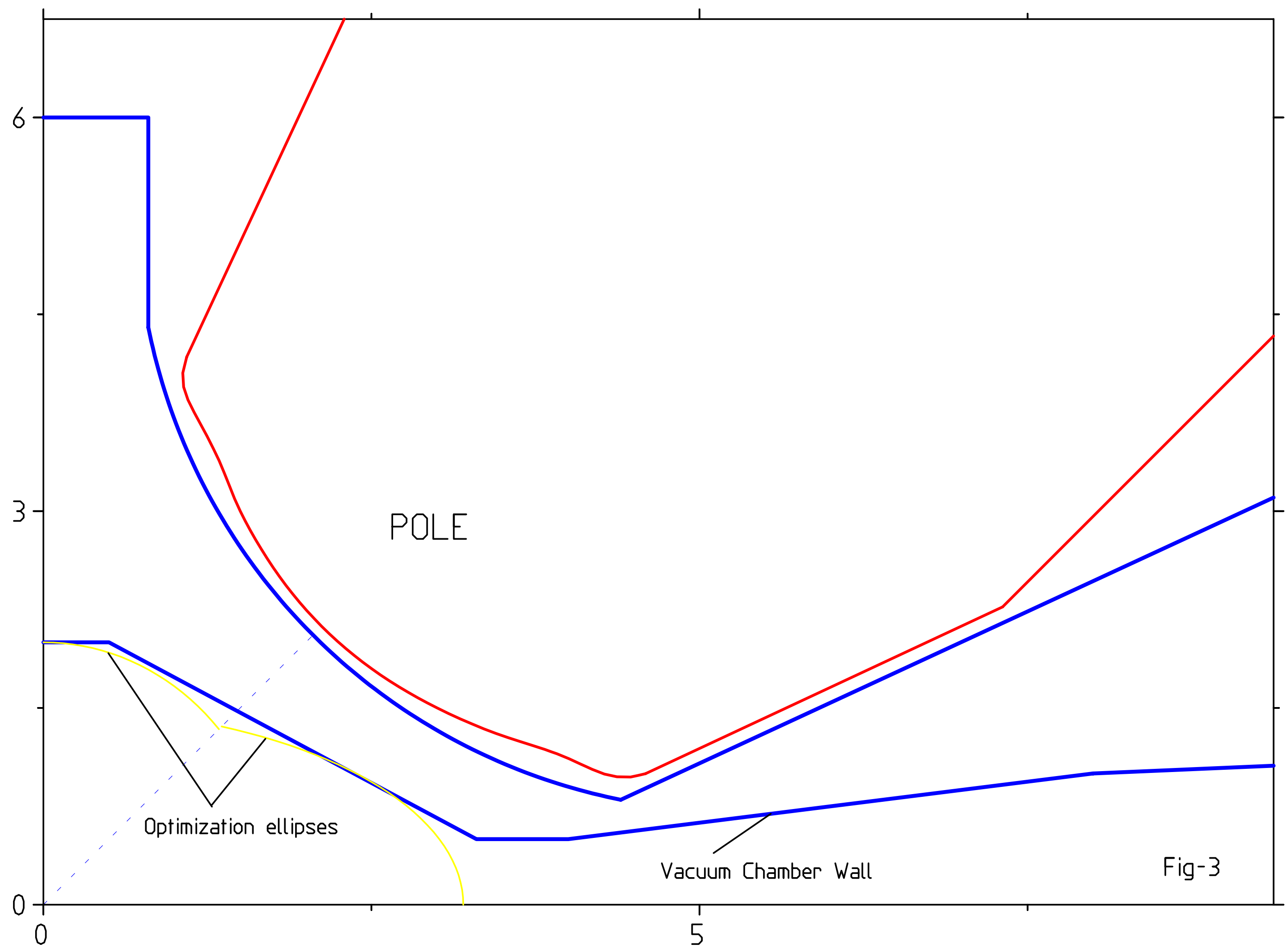

6
3
0
0
5
POLE
Optimization ellipses
Vacuum Chamber Wall
Fig-3

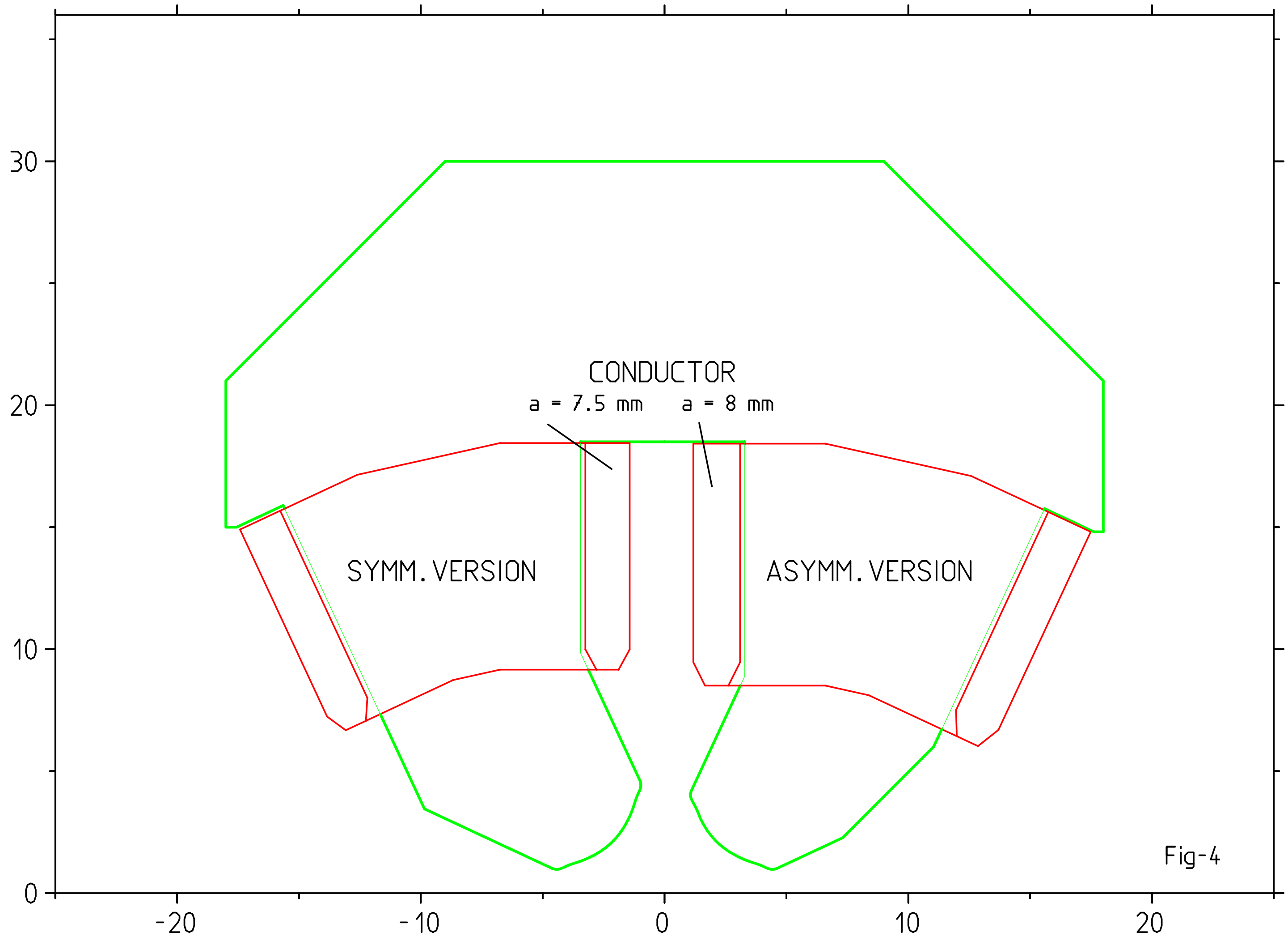
CONDUCTOR
a = 7.5 mm
a = 8 mm
SYMM. VERSION
ASYMM. VERSION
30
20
10
0
-20
-10
0
10
20

Fig-4

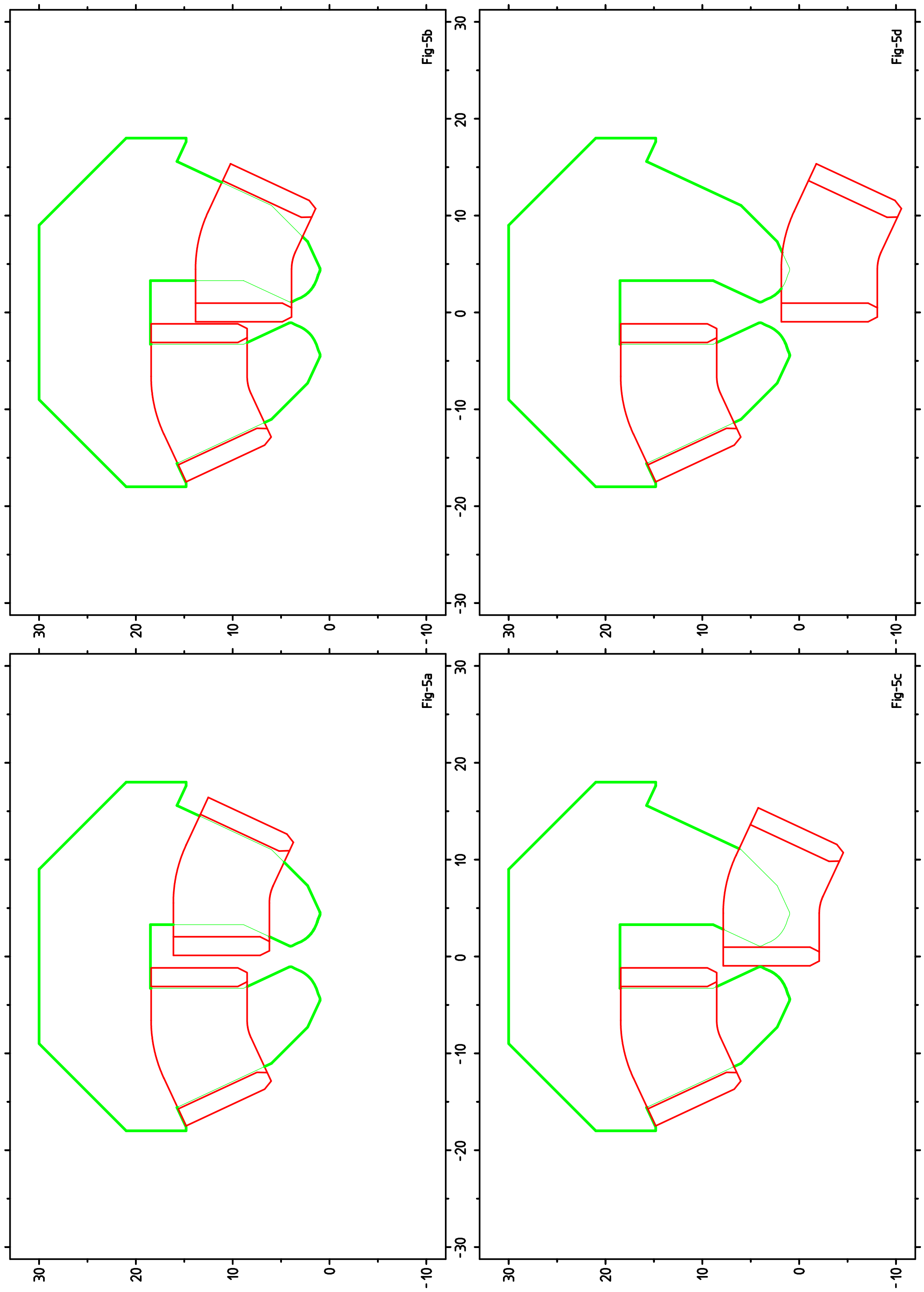
Fig-5a
Fig-5b
Fig-5c
Fig-5d
30
20
10
0
-10
-20
-30

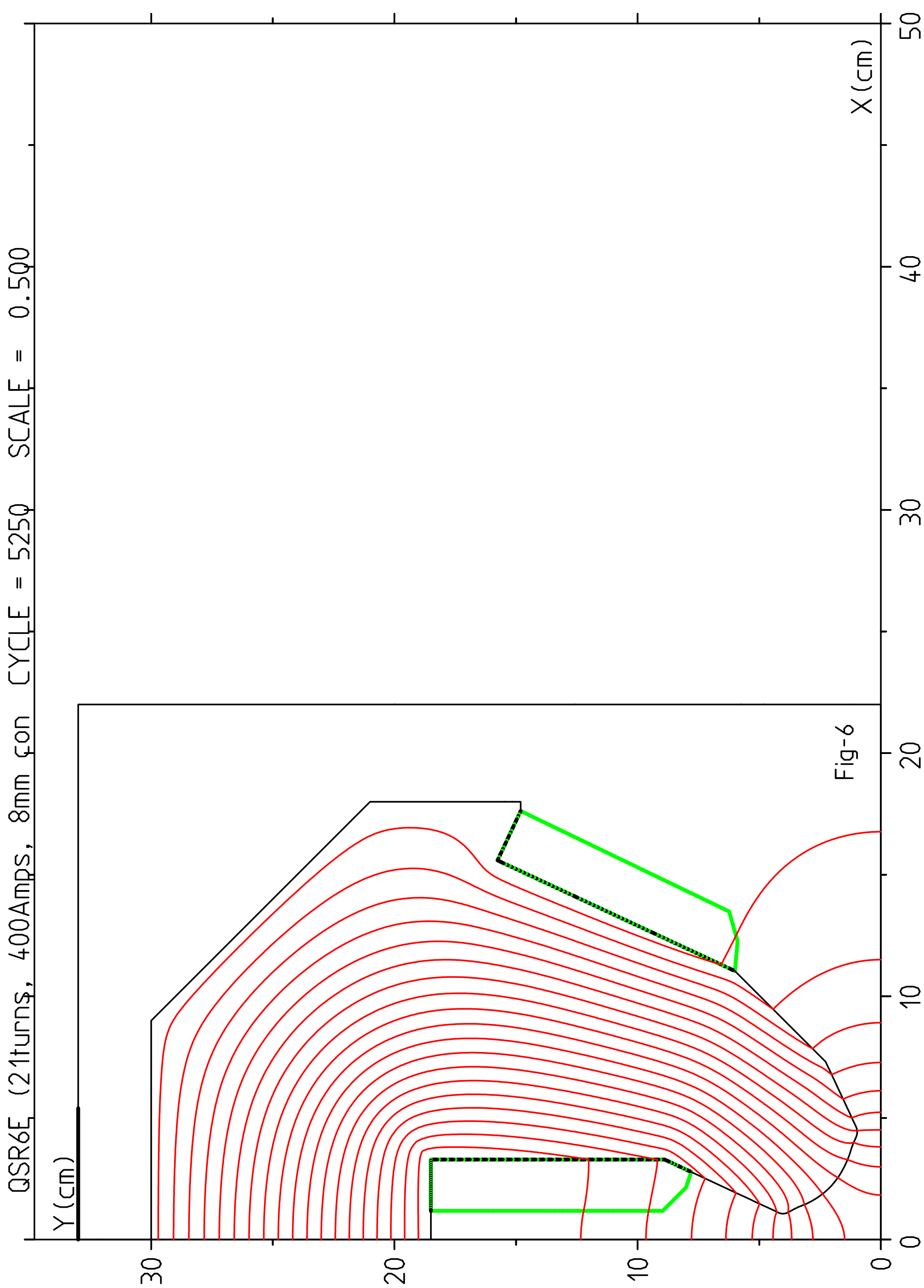
QSR6E (21turns, 400Amps, 8mm con CYCLE = 5250 SCALE = 0.500
Y (cm)
X (cm)
Fig-6
0
10
20
30
0
10
20
30
40
50

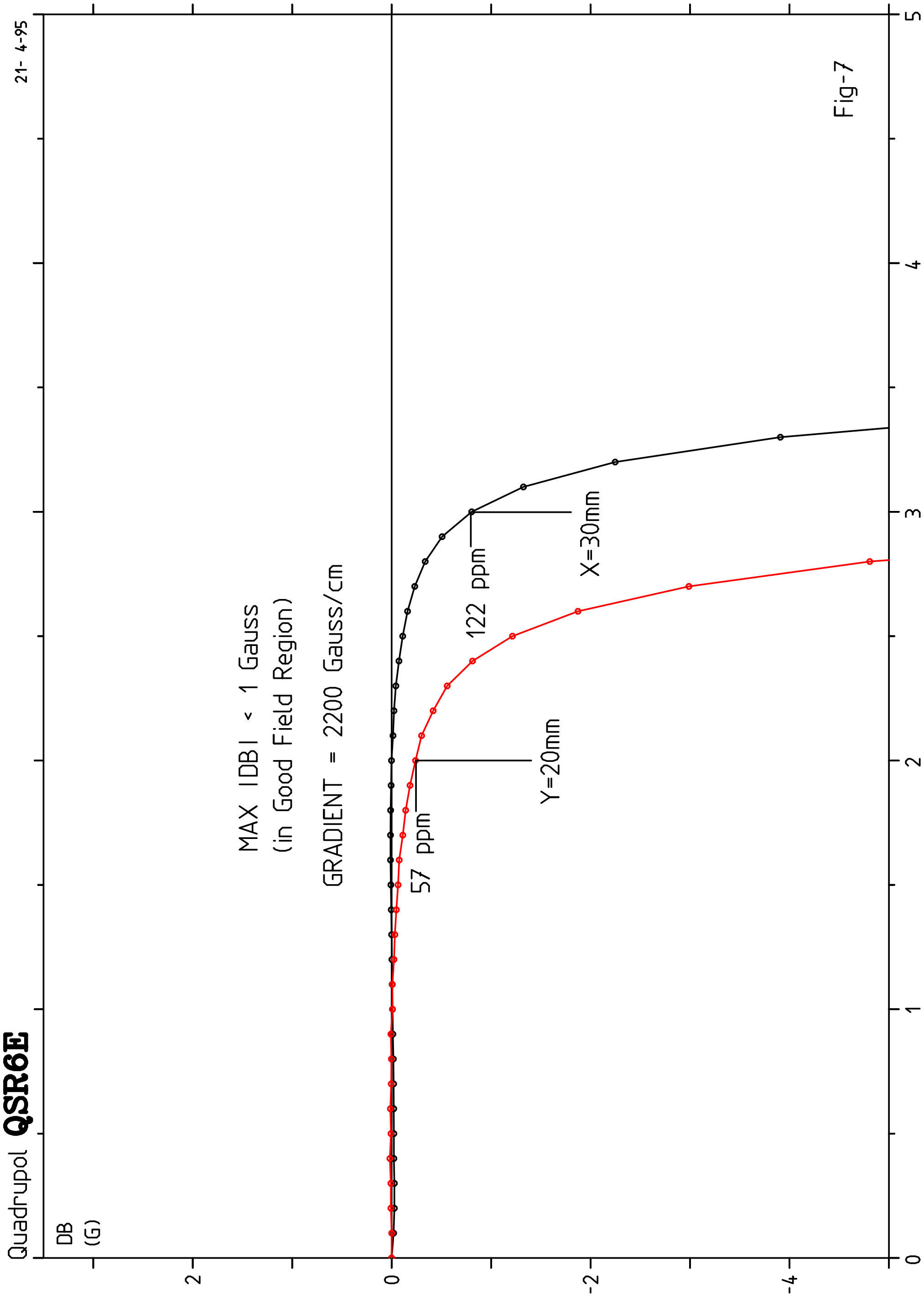

Quadrupol QSR6E
21- 4-95
DB
(G)
MAX |DB| < 1 Gauss
(in Good Field Region)
GRADIENT = 2200 Gauss/cm
122 ppm
X=30mm
57 ppm
Y=20mm
Fig-7
2
0
-2
-4
0
1
2
3
4
5

GRADIENT = 2200 Gauss/cm

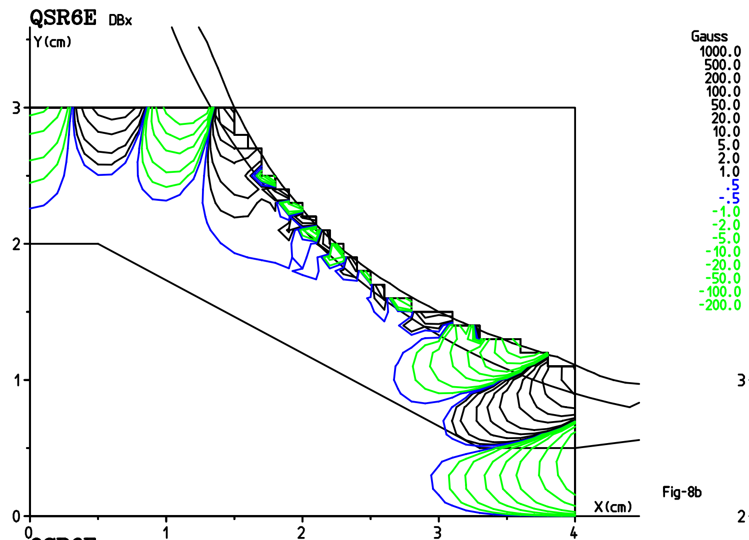

Fig-8b

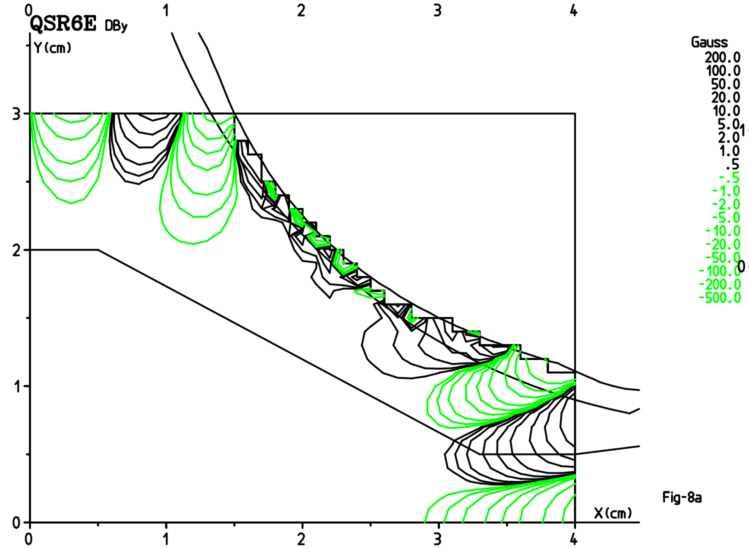

Fig-8a

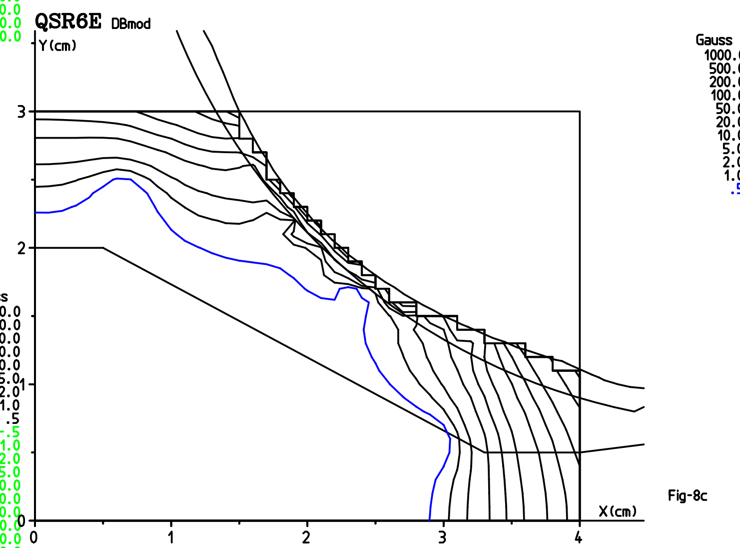

Fig-8c

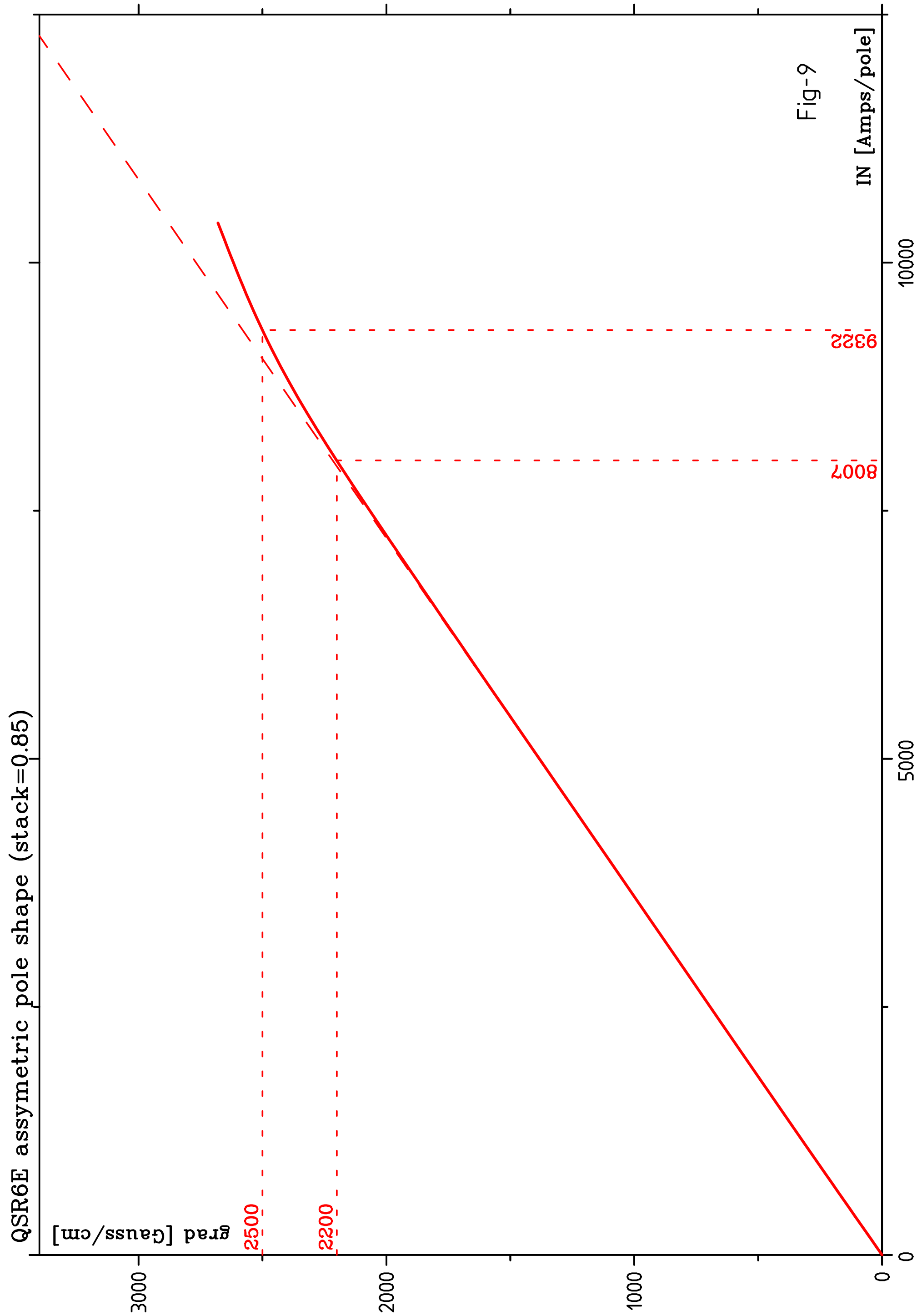
QSR6E assymetric pole shape (stack=0.85)
grad [Gauss/cm]
IN [Amps/pole]
Fig-9
2500
2200
8007
9322
0
1000
2000
3000
5000
10000

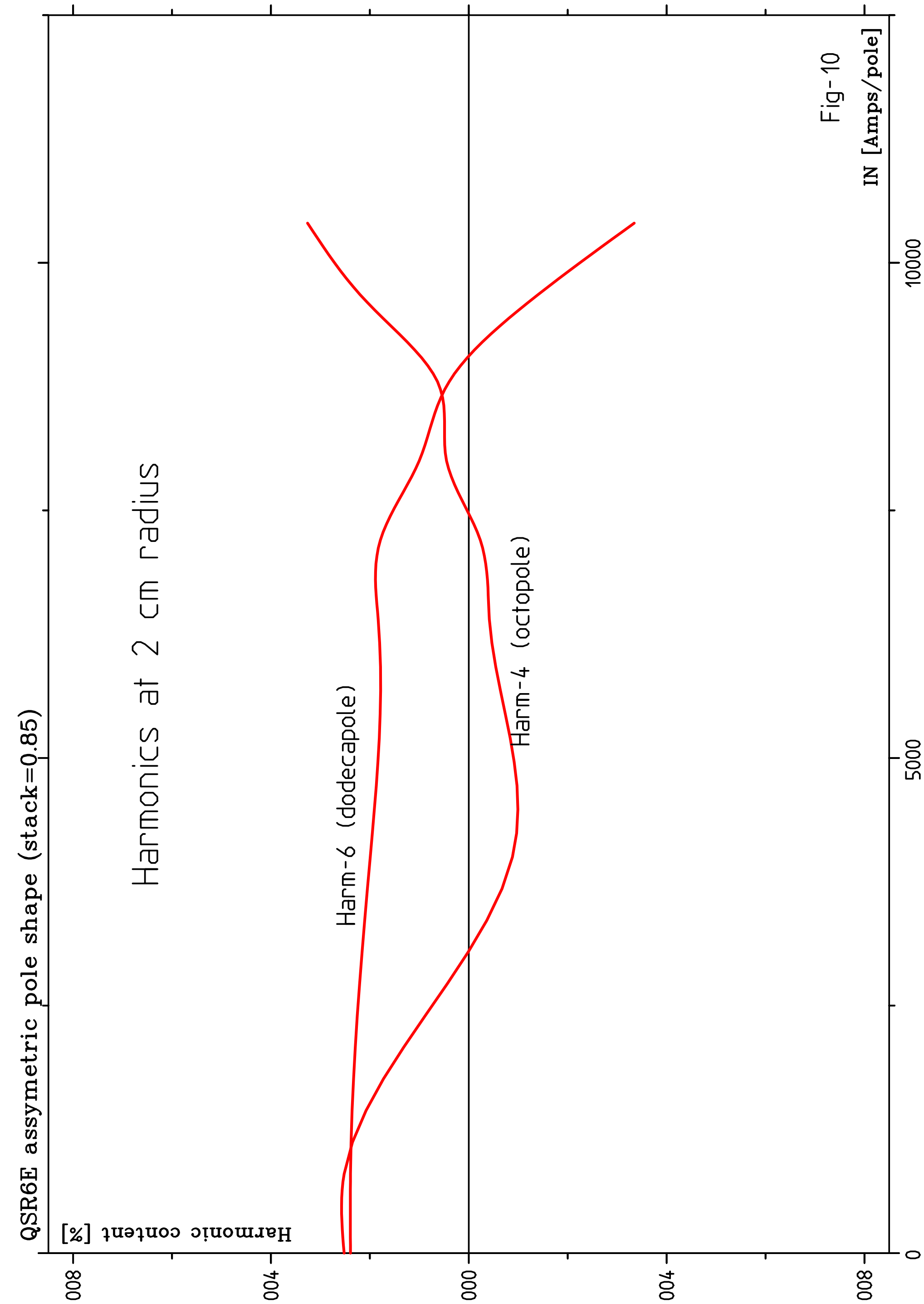
QSR6E assymetric pole shape (stack=0.85)
Harmonics at 2 cm radius
Harm-6 (dodecapole)
Harm-4 (octopole)
Harmonic content [%]
0.008
0.004
0.000
-0.004
-0.008
0
5000
10000
IN [Amps/pole]
Fig-10

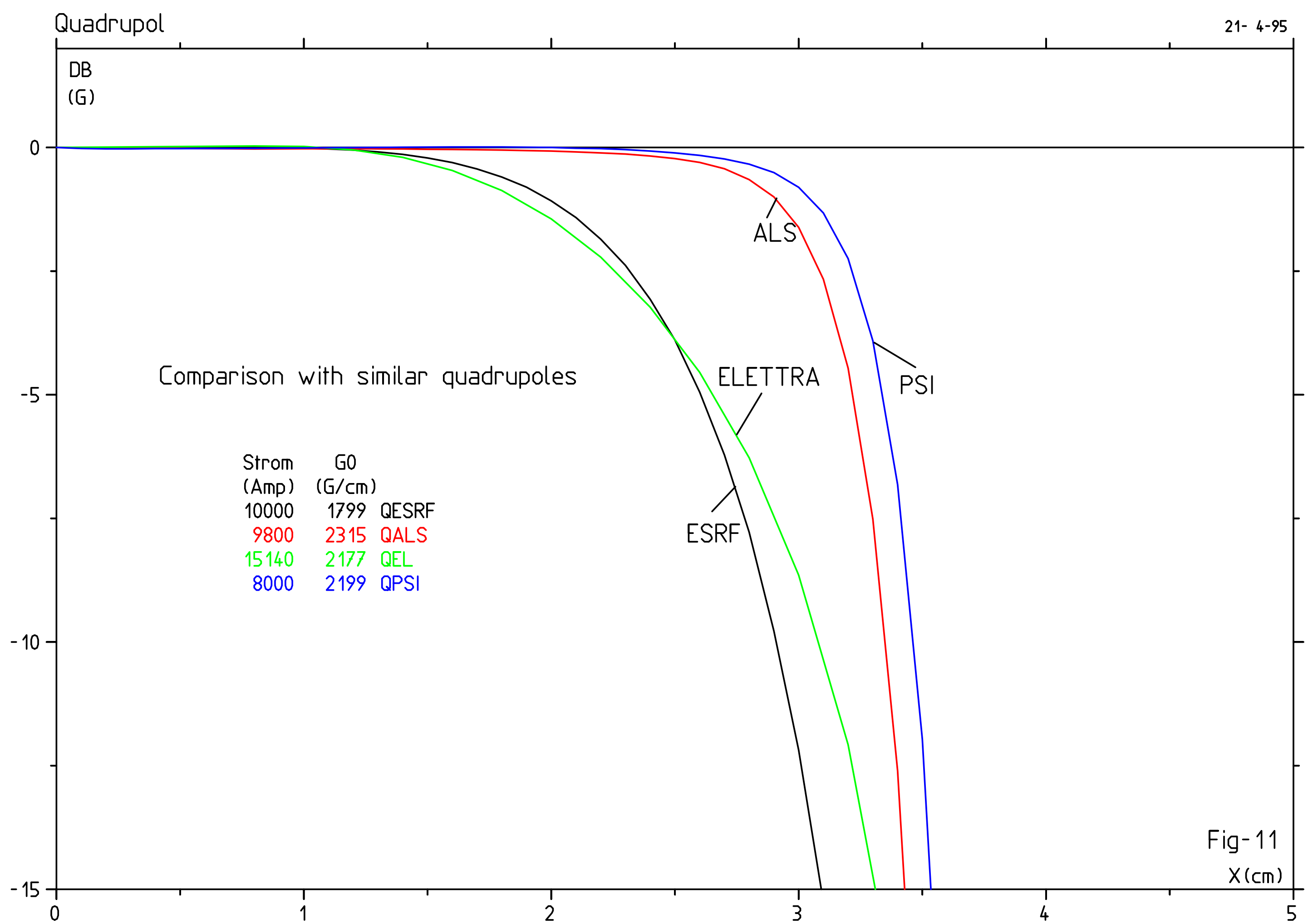
Quadrupol
21- 4-95
DB
(G)
0
-5
-10
-15
0
1
2
3
4
5
X(cm)
Fig-11
Comparison with similar quadrupoles
Strom (Amp) G0 (G/cm)
10000 1799 QESRF
9800 2315 QALS
15140 2177 QEL
8000 2199 QPSI
ALS
PSI
ELETTRA
ESRF